BMC Pulmonary Medicine

RESEARCH

Open Access

# Prognostic value and molecular mechanisms of OAS1 in lung adenocarcinoma

Lei Wang[1], Linlu Gao[1], Fei Ding[2], Kun Gao[1], Qian Liu[3] and Xiaoling Yin[4*]

## Abstract

**Background** The expression of 2′-5′-oligoadenylate synthetase 1 (OAS1) in lung cancer has been validated in numerous studies. However, the prognostic value of OAS1 expression in lung adenocarcinoma (LUAD) still remains unclear. This study aimed to reveal the prognostic value and associated molecular mechanisms of OAS1 expression in LUAD.

**Methods** Gene expression data of LUAD were extracted from online databases. Gene and protein expression levels of OAS1 in LUAD and normal samples were revealed, followed by prognostic analysis of OAS1. Next, we conducted a thorough bioinformatics analysis to examine the enrichment of key functional and biological signaling pathways and their correlation with the abundance of immune cells. The independent prognoses, drug responses, and PPI networks associated with OAS1 were analyzed. OAS1 expression was evaluated in LUAD tissues and cell lines. OAS1 was knocked down by siRNA transfection, followed by CCK8, colony formation, and wound-healing assays.

**Results** Gene and protein expression levels of OAS1 in LUAD samples were significantly higher than those in normal samples (all $P < 0.05$). OAS1 stimulation were correlated with poor prognosis, lymph node metastasis, advanced tumor stage, immune cells, and immunomodulators. The prognostic value of OAS1 in LUAD was determined via univariate regression analysis. In total, 10 OAS1-associated genes were revealed via PPI analysis of OAS1, which were primarily enriched in functions, such as the negative regulation of viral genome replication. Transcriptional analysis revealed several OAS1-related interactions, including STAT3-miR-21-OAS1. STAT3 was overexpressed and miR-21 was expressed in LUAD cells. Upregulation of OAS1 protein was determined in LUAD tissues and cell lines. OAS1 knockdown significantly reduced proliferation and migration of LUAD cells.

**Conclusions** OAS1 overexpression influenced survival and immune cell infiltration in patients with LUAD, which might be a potential prognostic gene for LUAD. Moreover, OAS1 contributed to LUAD progression by participating in STAT3-miR-21-OAS1 axis.

**Keywords** Lung adenocarcinoma, OAS1, Prognosis, Function and pathway, Transcription regulatory network

*Correspondence:
Xiaoling Yin
4048740@qq.com; DCxiaolingY@163.com
[1]Oncology Department, Zibo Hospital of Integrated Traditional Chinese and Western Medicine, Zibo City 255022, Shandong Province, China
[2]Oncology Department, Zibo First Hospital, Zibo City 255022, Shandong Province, China
[3]Oncology Department, Zibo City Hospital of Integrated Chinese and Western Medicine, Zibo City 255000, Shandong Province, China
[4]Respiratory Department, Zibo Hospital of Integrated Traditional Chinese and Western Medicine, No. 8, Jinjing Avenue, Zhangdian District, Zibo City 255022, Shandong Province, China

© The Author(s) 2024. **Open Access** This article is licensed under a Creative Commons Attribution-NonCommercial-NoDerivatives 4.0 International License, which permits any non-commercial use, sharing, distribution and reproduction in any medium or format, as long as you give appropriate credit to the original author(s) and the source, provide a link to the Creative Commons licence, and indicate if you modified the licensed material. You do not have permission under this licence to share adapted material derived from this article or parts of it. The images or other third party material in this article are included in the article's Creative Commons licence, unless indicated otherwise in a credit line to the material. If material is not included in the article's Creative Commons licence and your intended use is not permitted by statutory regulation or exceeds the permitted use, you will need to obtain permission directly from the copyright holder. To view a copy of this licence, visit http://creativecommons.org/licenses/by-nc-nd/4.0/.

## Background

Lung adenocarcinoma (LUAD) is a malignant tumor belonging to a subtype of non-small cell lung cancer [1]. Globally, millions of people are diagnosed with LUAD, and the high mortality rate associated with this disease poses a significant challenge to patients and the healthcare system [2]. LUAD diagnosis primarily relies on imaging and pathological examination; however, the accuracy and sensitivity of these methods are limited, particularly for early diagnosis [3, 4]. Therefore, the identification of new prognostic methods and biomarkers is vital for the clinical treatment of LUAD.

In LUAD, certain genes undergo mutations or aberrant expression, resulting in uncontrolled proliferation and metastasis of cancer cells [5]. Therefore, diagnostic genes have become a focus of research, as they can be used for early cancer detection, disease analysis, and guidance in the development of treatment plans [6, 7]. The 2'-5'-oligoadenylate synthetase 1 (OAS1) is a key gene involved in immune defense reactions [8]. It has been shown that OAS1 mutations primarily lead to the overall disruption of immune signaling pathways in human diseases, such as heart failure [9]. In recent years, research has demonstrated significant upregulation of OAS1 expression in pancreatic tumors, potentially implicating its prognostic value in cancer [10]. Based on TCGA database, Song et al. showed that OAS1 is an important immune-related gene that distinguishes between high- and low-risk patients with LUAD, indicating a promising prognostic role of OAS1 in LUAD [11]. Bioinformatics research plays a crucial role in elucidating the relationship between OAS1 and human cancer [12]. Through the analysis of extensive gene expression profiling data, potential mechanisms underlying the involvement of OAS1 in tumor development have been elucidated [13]. Despite the significant potential of OAS1 in the context of LUAD, a comprehensive understanding of its precise mechanisms and roles in the disease remains incomplete. Thus, further in-depth studies are required to determine the role of OAS1 in the prognosis and development of LUAD.

In this study, we aimed to address the prognostic value of OAS1 in LUAD using bioinformatics approaches. The integration of these findings with clinical parameters was used to enhance risk stratification and guide therapeutic decisions, which further unraveled the intricate relationship between OAS1 expression and LUAD pathophysiology. This study not only aimed to understand the role of OAS1 in LUAD but also provide new molecular markers for the clinical prognosis of LUAD.

## Methods

### Microarray data

TCG-LUAD RNA-seq data were downloaded from the UCSC Xene database [14]. The samples' survival prognosis information and clinical information, including age, sex, and pathologic_M, pathologic_N, pathologic_T, neoplasm_cancer_status, and tumor_stage, were downloaded. Moreover, LUAD microarray datasets, including GSE31210 [15] and GSE68465 [16] in the GEO database, were acquired for the current analysis. GSE31210 contains 20 normal samples (normal group) and 226 LUAD tumor samples (LUAD group) with prognostic information. GSE68465 contains 19 normal samples (normal group) and 443 LUAD tumor samples (tumor group) with prognostic information. Probes that did not correspond to gene symbols in the annotation file were excluded from the expression matrix. When multiple probes corresponded to the same gene, the average value of these probes was computed to represent the expression level of that gene. Finally, the expression value of OAS1 was extracted from each dataset for subsequent analyses.

### Gene and protein expression analyses of OAS1

OAS1 expression in all three datasets was analyzed using ggplot2 (version 3.4.0) in R [17]. The P value between the normal and LUAD groups was calculated using the Wilcoxon test. The results were visualized using a violin plot. To confirm the differential protein expression of OAS1, we used the HPA database [18], which provides comprehensive information on protein expression in various human tissues and organs using transcriptomics and proteomic techniques. We used the HPA database to examine the immunohistochemical levels of the OAS1 protein in LUAD.

### Survival investigation and clinical correlation exploration

The samples in all three datasets were separated into two groups according to survival information and OAS1 expression in the tumor samples, followed by the Kaplan–Meier test [19]. Finally, the candidate gene with the log-rank test ($P<0.05$) was enrolled as a prognostic gene for OS. Furthermore, based on the clinical characteristics of tumor samples from the TCGA-LUAD dataset, box plots of OAS1 gene expression were plotted among different clinical groups and significance was calculated using the inter-group Wilcoxon test. Moreover, the tumor specimens were divided into high- and low-expression groups using the median OAS1 expression value as the threshold. Finally, the correlation between different groups and clinical information was analyzed using the chi-squared test.

### Enrichment analysis of OAS1

The LinkFinder algorithm in LinkedOmics was used to analyze OAS1-associated genes in LUAD based on the Pearson correlation coefficient method. TOP50 genes positively and negatively correlated with OAS1 expression were visualized using a heatmap. In addition, KEGG

and GO enrichment analyses were used to obtain a scoring matrix using the GSVA algorithm (version 1.36.2) [20]. The most significant positive and negative correlations were identified as the TOP 25 significant results with a threshold of adjusted $P<0.05$, and redundancy was removed using affinity promotion and weighted set cover methods to obtain the final results for the bar graph display.

#### Immune cell infiltration investigation

To explore the disparities in the tumor microenvironment between the two risk groups, we employed CIBERSORT algorithms [21, 22] to estimate the infiltration levels of 22 types of immune cells, including memory B cells, CD8 T cells, and M2 macrophages, in TCGA-LUAD samples. The results were visually presented using box plots. Furthermore, we utilized the Spearman method to assess the correlation between immune-infiltrating cells and OAS1 ($p<0.05$) based on the cor algorithms in the R software (version 3.6.1). The Wilcoxon signed-rank test was used to detect significant differences (P values) in the immune cell populations between the groups. The outcomes were visually illustrated using Lollipop chart.

#### Correlation analysis between OAS1 and immune modulators

To determine the association between the immune system and LUAD progression, the correlation between OAS1 expression and immune modulators (including immunostimulators and immunosuppressants) was investigated using the TISIDB database [23]. The immunostimulators and immunosuppressants that were most significantly correlated (including positive and negative correlations) with OAS1 in patients with LUAD were selected and visualized using scatter plots.

#### Independent diagnostic analysis of OAS1

The independence of the diagnosis based on clinical factors and survival information (such as OS and OS.time) was explored using univariate and multivariate Cox regression analyses with the survival package in R software (version 3.6.1) [24] with $P<0.05$. These analyses aimed to determine whether OAS1 retained its significance after accounting for the influences of these variables.

#### Drug sensitivity analysis of OAS1

The Cancer Drug Sensitivity Genomics database was used to assess the sensitivity to chemotherapy drugs. The difference in sensitivity (IC50 value difference) for 138 chemotherapeutic drugs, and OAS1 expression was quantified using the pRRophic algorithm [25]. Spearman's correlation coefficient ($P<0.05$) was used to determine whether the difference in the IC50 value of each drug was associated with the OAS1. The results were visualized using a scatter plot.

#### PPI network investigation

Using the STING database (version 11.0, species: *Homo sapiens*), we extracted information on OAS1-associated protein interactions, revealing relationships among these proteins based on a score threshold (medium confidence) of 0.4. Subsequently, a network was constructed using Cytoscape (version 3.6.1) [26]. Additionally, we conducted GO and KEGG pathway enrichment analyses using the DAVID tool [27]. In the present study, the GO functions and KEGG pathways enriched with OAS1 and its associated proteins were investigated. $P<0.05$ was considered as thresholds.

#### The transcription regulatory network prediction

The transcription factors (TFs) that regulated OAS1 were investigated using the online software TRRUST (version 2). Then, the miRWalk 3.0 software [28] was selected as default databases for miRNA-OAS1 interaction scanning (binding probability ≥ 0.95; binding site position: 3UTR). Finally, common miRNA-mRNA interactions in databases, including miRDB (http://www.mirdb.org/) [29] and miRWalk 3.0, were enrolled for further investigation. The transcriptional regulatory network, including miRNA-OAS1 and TF-OAS1 interactions, was constructed using Cytoscape software (version: 3.4.0) [30].

#### Patients and tissue collection

Patients with LUAD were recruited from a hospital. Participants who did not present with chronic disorders and did not receive anti-tumor treatments were included. Tumor tissues and adjacent normal controls were collected from patients undergoing surgery. All participants provided written informed consent before commencement of the study. This study was approved by the Ethics Committee of our hospital (No.202211) and was conducted in accordance with the Declaration of Helsinki guidelines. This study was registered in Chictr.org.cn (https://www.chictr.org.cn/) with Clinical Trial Number of ChiCTR2400085823.

#### Immunohistochemical staining

The lung tissues were fixed in 4% paraformaldehyde and embedded in paraffin. The consecutive tissue sections at 4 μm were prepared. After deparaffinization and rehydration, sections were blocked with skim milk. CD68 immunostaining was used for M1 macrophages as described in the previous study [31]. The antibodies used in immunostaining included OAS1 rabbit monoclonal antibody (1:500, Abcam), CD68 rabbit monoclonal antibody (1:500, Abcam), and goat anti-rabbit IgG secondary

antibodies (1:800, Abcam). Finally, the proteins were visualized using diaminobenzidine and hematoxylin staining. ImageJ software was used for quantitative analysis. The protein expression of OAS1 was evaluated using a 0–4 scoring scale based on the area of positive staining and staining intensity [10]. A score of 0, 1, 2 indicated low expression, while a higher score indicated high expression.

#### RT-qPCR assay

Four human LUAD cell lines (A549, NCI-H78, NCI-H102, and BL2195) and a normal bronchial epithelial cell line, BEAS-2B, were purchased from the Cell Bank of the Chinese Academy of Sciences (Shanghai, China). We utilized a combination of Roswell Park Memorial Institute (RPMI) 1640 medium and fetal bovine serum, both sourced from Hyclone in the USA, with a final concentration of 10% fetal bovine serum for cell culture experiments, and cultured at 37 ˚C with 5% $CO_2$. Total RNA was isolated from LUAD cell lines and normal control cells using TRIZOL reagent (Invitrogen, USA), and reverse transcription was conducted using the RevertAid First Strand cDNA Synthesis Kit (Thermo Fisher Scientific). PCR was performed on an ABI7500 (Applied Biosystems, U.S.A.) with GAPDH as the internal reference. The primers were synthesized by Sangon Biotech (Shanghai, China). Information for all sequences is shown in Table 1. The PCR program were as follows: 95 °C for 4 min, 40 cycles of 95 °C for 30 s, and 50 °C for 30s. The relative expression was calculated using the $2^{-\Delta\Delta Ct}$ method [32].

#### Western blot

The protein expression of OAS1 in LUAD cell lines was detected using western blot analysis. Briefly, proteins were extracted from A549 and NCI-78 cells and from normal controls. Proteins were separated via sodium dodecyl sulfate-polyacrylamide gel electrophoresis and transferred onto PVDF members. After the membranes were treated with 10% fetal calf serum, the proteins in each group were incubated with OAS1 rabbit monoclonal primary antibody (1:1000, Abcam), followed by goat anti-rabbit IgG secondary antibody (1:5000, Abcam). Finally, ECL reagent was used for staining, and the proteins were quantitatively analyzed using ImageJ software.

**Table 1** The detail information for all primers used in current study

| Primer | Sequence(5′-3′) |
|---|---|
| OAS1-F | ACCTGAGAAGGCAGCTCACGAAAC |
| OAS1-R | CAGGGAGGAAGCAGGAGGTCTCAC |
| STAT3-F | CACCAAGCGAGGACTGAGCAT |
| STAT3-R | GCCAGACCCAGAAGGAGAAGC |
| miR-21-F | ACACTCCAGCTGGGTAGCTTATCAGACTGA |
| miR-21-R | GTGTCGTGGAGTCGGCAA TTC |
| GAPDH-F | CAAGGTCATCCATGACAACTTCG |
| GAPDH-R | GTCCACCACCCTGTTGCTGTAG |
| U6-F | GCGCGTCGTGAAGCGTTC |
| U6-R | GTGCAGGGTCCGAGGT |

*Notes*: OAS1, 2′-5′-Oligoadenylate Synthetase 1; GAPDH, Glyceraldehyde 3-phosphate dehydrogenase

#### OAS1 knockdown

Small interfering RNA (siRNA) targeting OAS1 and the corresponding control (siNC) were synthesized by Shanghai GeneChem Co., Ltd. A549 cells were seeded onto 24-well plates and cultured overnight. When the cells attained 30% confluence, si-OAS1 and siNC were transferred into the cells using Lipofectamine 2000. After 24 h of transfection, the cells were collected and the transfection efficiency was determined using RT-qPCR.

#### Cell viability detection

Changes in cell viability following OAS1 knockdown were detected using a CCK8 assay kit (Solarbio, Beijing, China). Cell suspension (100 μL/well) was plated on a 96-well plate and incubated for 24 h, 48 h, and 72 h at 37℃ in an incubator with 5% CO2. Next, 10 μL CCK8 solution was added in each cell culture and maintained for 2 h. Finally, the absorbance value (OD) at 450 nm was measured with the implementation of a microplate reader.

#### Colony formation assay

Cells at logarithmic phase were digested with 0.25% trypsin to prepare a single-cell suspension. Next, the cells were seeded in 6-well plates (700 cells/well) and cultured in complete medium with 10% fetal calf serum. After 10 d of cell culture, 1% crystal violet was used for colony staining. The cell colonies were observed and captured under an inverted light microscope equipped with a camera.

#### Statistical analysis

GraphPad prism 8.0 was employed for statistical analysis and graphs making. The data were expressed as mean ± standard deviation (SD). The between group and multiple group comparison were conducted using t test and one-way ANOVA method, respectively. A difference of $p < 0.05$ was considered statistically significant.

## Results

#### Expression analysis of OAS1

The gene expression values of OAS1 were extracted from TCGA-LUAD (Fig. 1A), GSE31210 (Fig. 1B), and GSE68465 datasets (Fig. 1C). OAS1 expression was dramatically increased in the tumor group compared to that in the normal group in all three datasets, incorporating sample grouping information. Moreover, the results of protein immunostaining for OAS1 in LUAD (Fig. 1D)

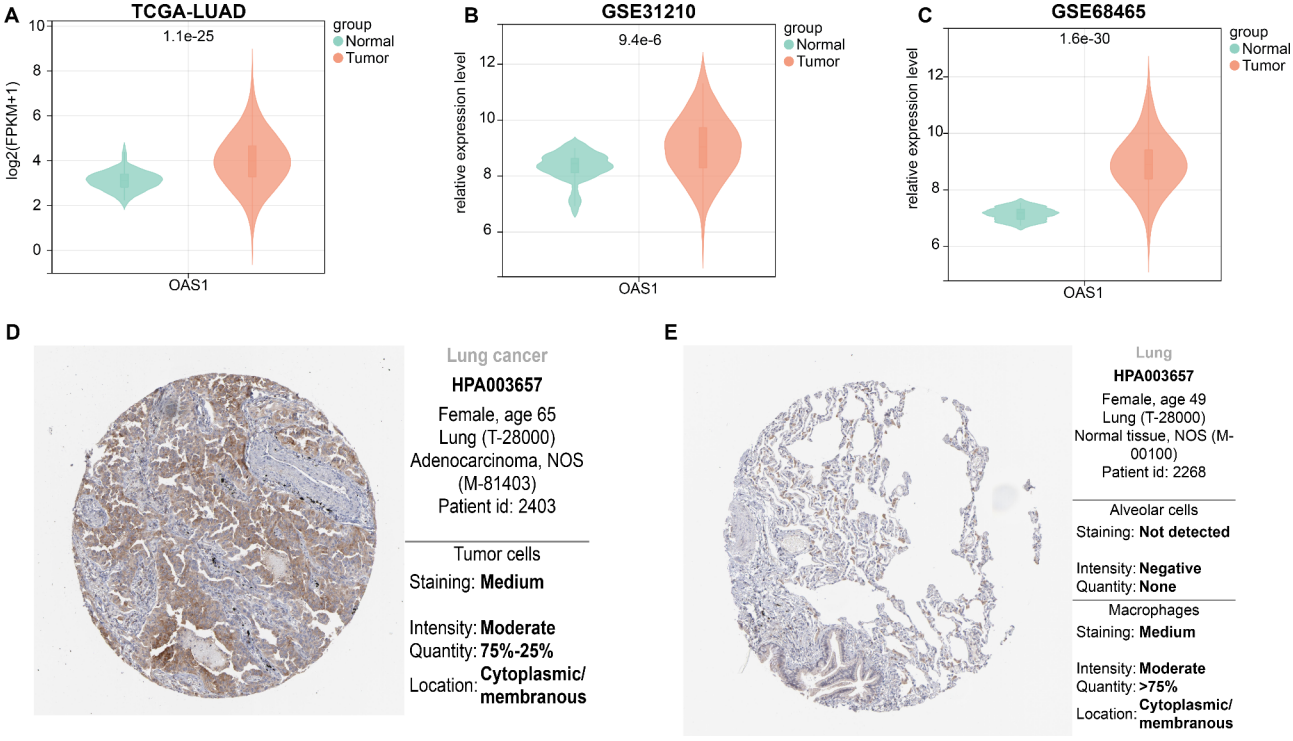


**Fig. 1** The OAS1 gene and associated protein expression in normal lung samples and Lung Adenocarcinoma (LUAD) samples. (**A**), the violin chart showed the expression of OAS1 between normal samples and LUAD samples from TCGA-LUAD dataset. (**B**), the violin chart showed the expression of OAS1 between normal samples and LUAD samples from GSE31210 dataset. (**C**), the violin chart showed the expression of OAS1 between normal samples and LUAD samples from GSE68465 dataset. (**E**), the protein immunostaining of OAS1 in LUAD. (**F**), the protein immunostaining of OAS1 in normal Lung tissues

and normal lung tissues (Fig. 1E) indicated that OAS1 protein in LUAD was elevated when compared to that in the normal lung tissue.

### Survival and clinical correlation analysis of OAS1

Based on survival confirmation, all samples were assigned to two different groups based on the median score of OAS1 expression in TCGA-LUAD (Fig. 2A), GSE31210 (Fig. 2B), and GSE68465 (Fig. 2C). Compared with the low-expression group, survival in the high-expression group was worse in all three datasets. Moreover, expression analysis of OAS1 among the different clinical characteristics of tumor samples from TCGA-LUAD dataset showed that pathologic_N (Fig. 2D), tumor_stage (Fig. 2E), and neoplasm_cancer_status (Fig. 2F) were closely associated with OAS1 expression (Supplementary Fig. 1). The significance between different OAS1 expression groups and clinical factors determined using the chi-square test is listed in Supplementary Table 1. The results showed that pathologic N, pathologic T, and tumor stage were significantly related to OAS1 expression (all $P<0.05$).

### Enrichment analysis of OAS1-associated genes

The OAS1-associated genes in LUAD were investigated in this study (Supplementary Fig. 2). The heat maps for the TOP50 genes that were positively and negatively correlated with OAS1 are shown in Fig. 3A and B, respectively. Moreover, gene set enrichment analysis showed that the TOP 25 genes that were positively and negatively correlated with OAS1 mainly assembled in GO functions, such as response to type I interferon (BP, GO:0034340) (Fig. 3C), peptidase complex (CC, GO:0000793) (Fig. 3D), and double-stranded RNA binding (MF, GO:0003725) (Fig. 3E). These genes were mainly enriched in the measles (hsa05162) and cGMP-PKG signaling pathways (hsa04022) (Fig. 3F).

### Immune-associated analysis of OAS1

All samples were separated into an overexpression (H-OAS1) group and a low-expression (L-OAS1) group, based on the expression values of OAS1 in the tumor samples. Compared with the L-OAS1 group, the percentages of plasma cells and CD4 memory resting T cells were dramatically decreased in the H-OAS1 group (all $P<0.05$), whereas activated CD4 memory T cells, T cell gamma delta, macrophages M0, macrophages M1, and activated dendritic cells were significantly increased

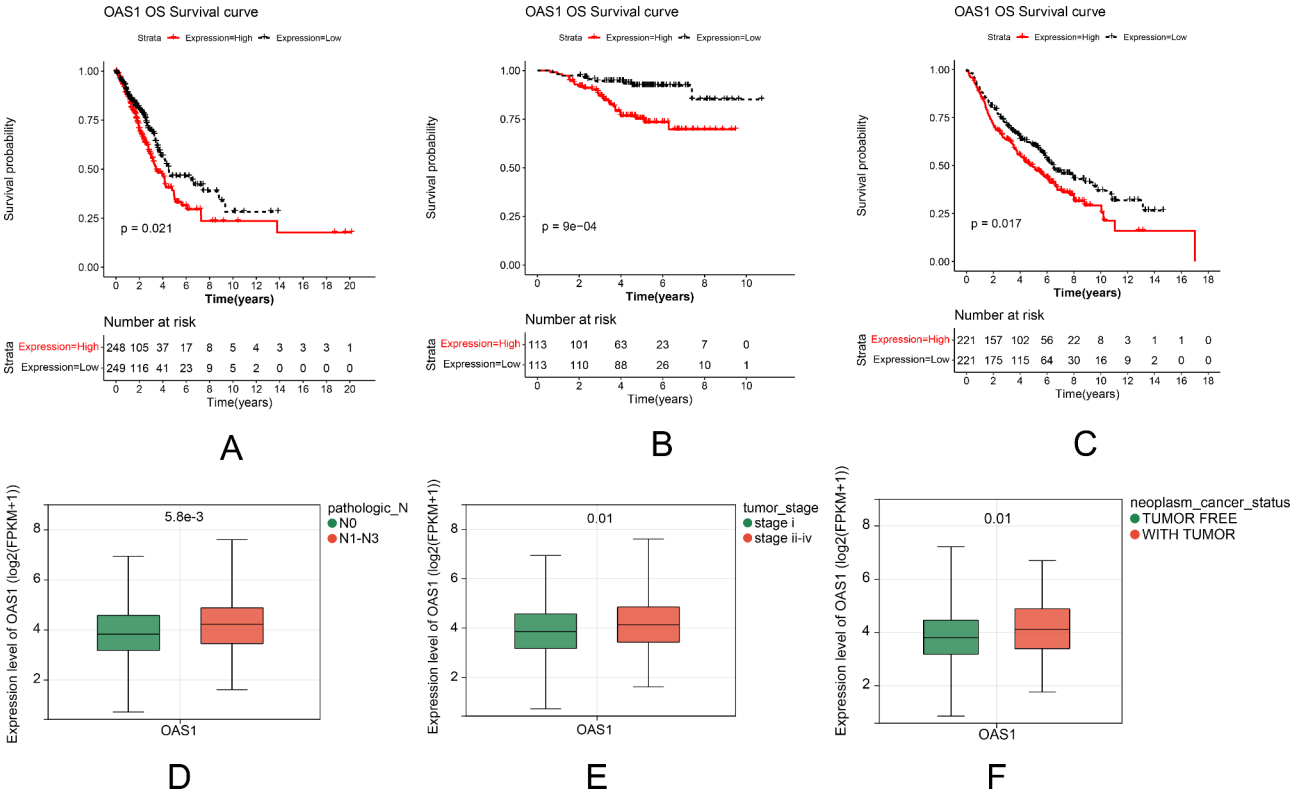


**Fig. 2** The OAS1 expression related to survival and clinical characteristics. (**A**), K-M analysis revealed the correlation between OAS1 expression and survival of LUAD patients based on TCGA-LUAD dataset. (**B**), K-M analysis revealed the correlation between OAS1 expression and survival of LUAD patients based on GSE31210 dataset. (**C**), K-M analysis revealed the correlation between OAS1 expression and survival of LUAD patients based on GSE68465 dataset. (**D**), the expression of OAS1 was significantly correlated with pathologic_N based on TCGA-LUAD dataset. (**E**), the expression of OAS1 was significantly correlated with tumor_stage based on TCGA-LUAD dataset. (**F**), the expression of OAS1 was significantly correlated with neoplasm_cancer_statusbased on TCGA-LUAD dataset. The top number in D-F represented P value

in the H-OAS1 group (all $P<0.05$) (Fig. 4A). These findings indicated distinct immune cell profiles associated with the different groups. Spearman software was used to evaluate the correlation between OAS1 expression and the number of immune-infiltrating cells. According to the lollipop chart (Fig. 4B), the expression of OAS1 exhibited a statistically significant positive correlation with activated dendritic cells, macrophages M0, T cells gamma delta, T cells CD4 memory activated, and macrophages M1. Conversely, it demonstrated a negative correlation with CD4 memory T cell resetting, dendritic cell resetting, monocytes, plasma cells, and activated mast cells (all $p<0.05$). Based on the TISIDB database, the correlation between OAS1 and immune modulators, including immunostimulants (Fig. 4C) and immunosuppressants (Fig. 4D), was further investigated. The results showed that the two immunostimulants, RAET1E (Fig. 4E) and IL6R (Fig. 4F), were significantly correlated with OAS1 expression. Two immunosuppressants, LGALS9 (Fig. 4G) and ADORA2A (Fig. 4H), showed the strongest correlation with OAS1 expression.

### Independent prognostic analysis

Prognostic analysis based on OAS1 and six clinical factors revealed by univariate Cox regression showed that OAS1, pathologicM, pathologicN, pathologicT, and tumor stage were closely related to survival. Multivariate Cox regression analysis based on OAS1 and the four clinical factors (pathologic_M, pathologic_N, pathologic_T and tumor stage) revealed that OAS1 and tumor stage were the independent prognostic factors for LUAD (Supplementary Table 2).

### Drug and PPI analysis of OAS1

Based on the TCGA-LUAD dataset, the IC50 values of the drugs associated with OAS1 expression were determined. The results showed a close association between the IC50 values of the 80 drugs and OAS1 expression (all $P<0.05$). Paclitaxel exhibited an inverse correlation with OAS1 expression (Fig. 5A), whereas imatinib displayed a positive correlation with OAS1 expression (Fig. 5B). A PPI network was established using 11 nodes, including OAS1 and associated 10 proteins (Fig. 5C). These node genes were mainly assembled in GO-BP functions, such as negative regulation of viral genome replication

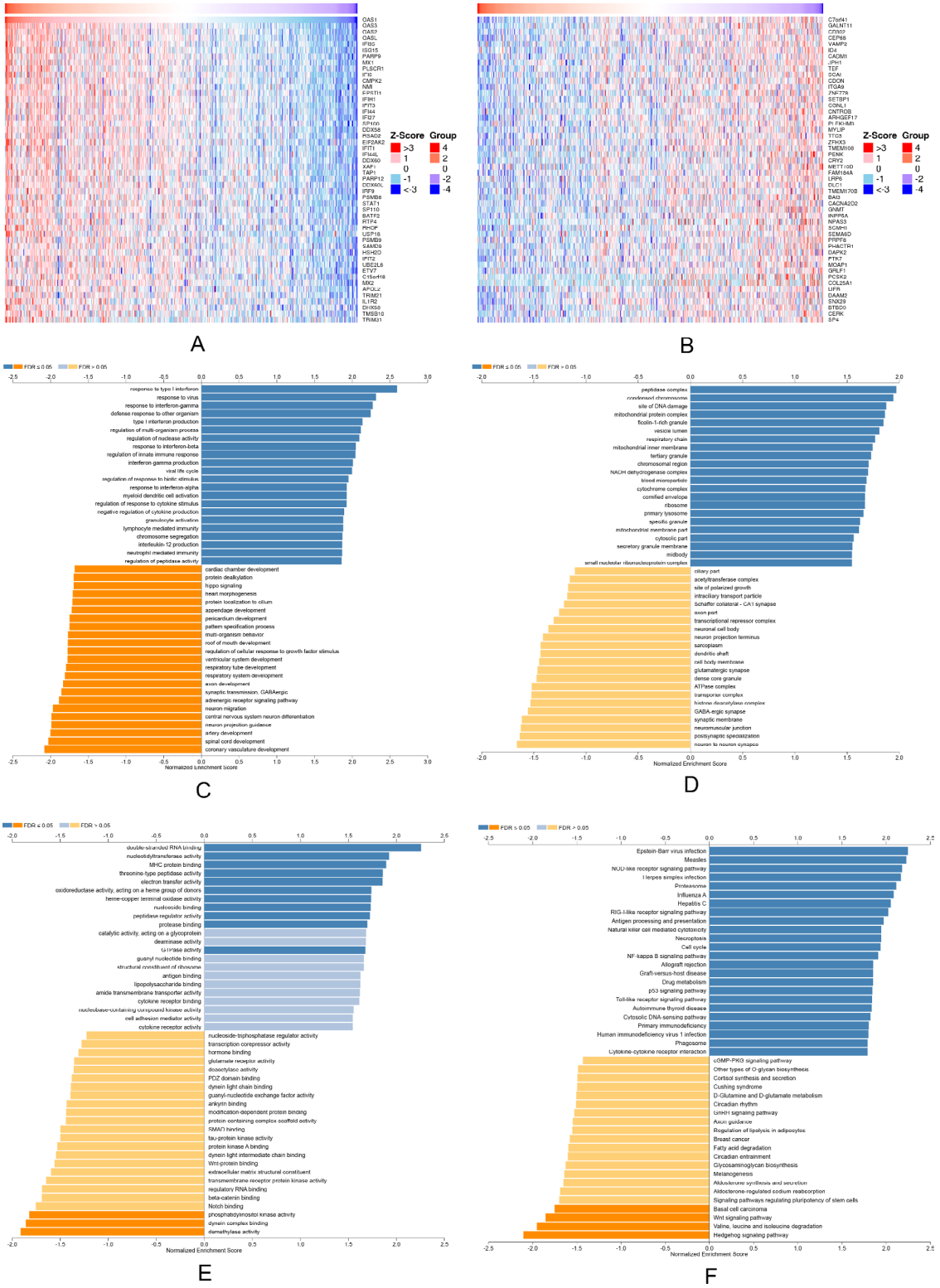


**Fig. 3** The TOP 50 OAS1 related genes and associated GSEA enrichment analysis. (**A**), the heat map showed TOP 50 genes that positively correlated with OAS1. (**B**), the heat map showed TOP 50 genes that negatively correlated with OAS1. (**C**), the TOP 25 GO-BP functions assembled by that OAS1 related positively and negatively genes respectively. (**D**), the TOP 25 GO-CC functions assembled by that OAS1 related positively and negatively genes respectively. (**E**), the TOP 25 GO-MF functions assembled by that OAS1 related positively and negatively genes respectively. (**F**), the TOP 25 KEGG pathways enriched by that OAS1 related positively and negatively genes respectively

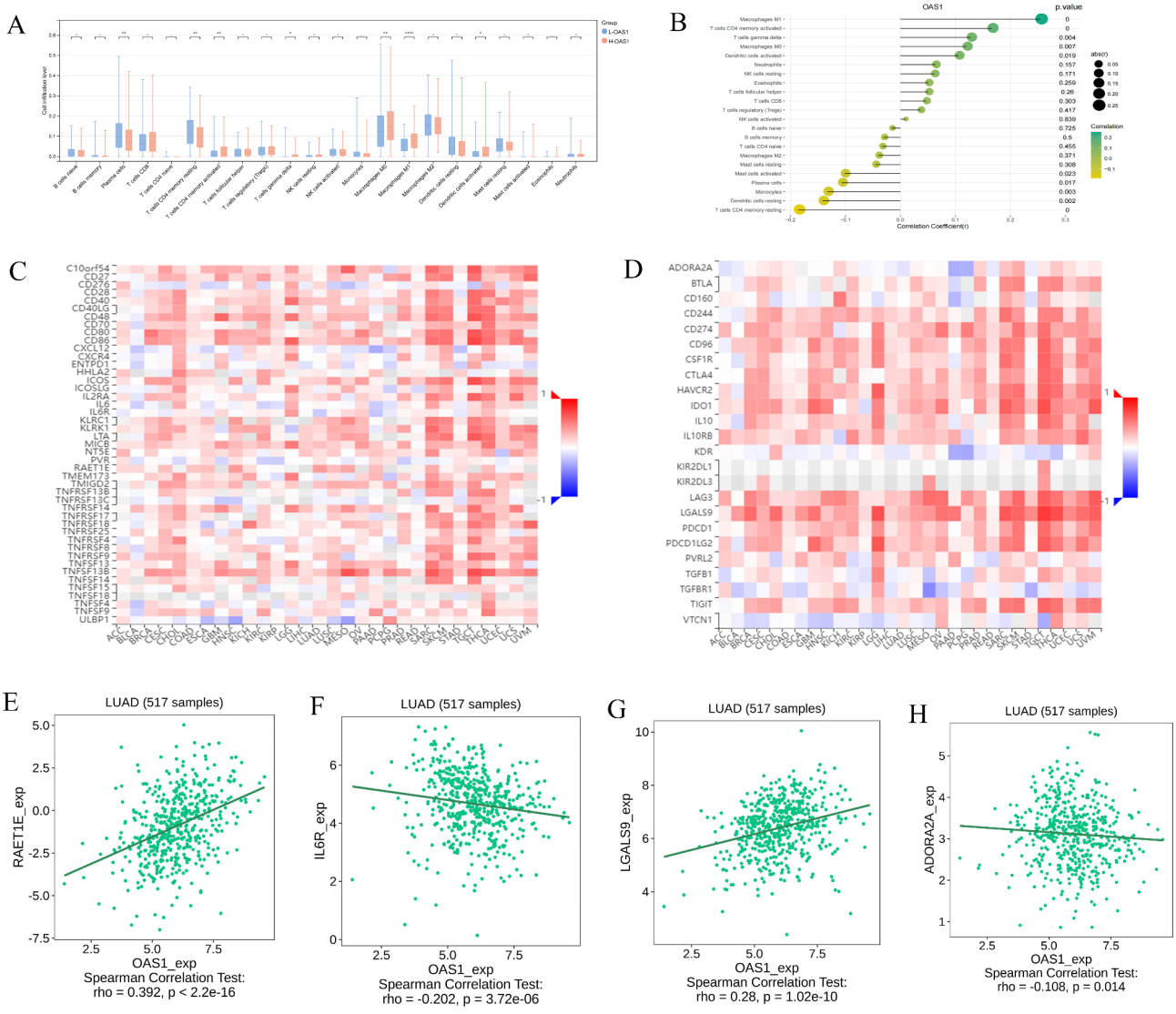


**Fig. 4** Immune associated analysis for OAS1 in current study. (**A**), the immune cell infiltration analysis based on immune cells and OAS1 expression: L-OAS1, low expression group of OAS1; H-OAS1, high expression group of OAS1; *, $P<0.05$; **, $P<0.01$; ***, $P<0.001$. (**B**), Spearman correlation lollipop map revealed the correlation between 22 immune cell infiltration and OAS1 gene expression. (**C**), correlation heatmap between OAS1 and immunestimulators: X-axis represented different types of cancer, while Y-axis represented the gene symbol of immunestimulators. (**D**), correlation heatmap between OAS1 and immunosuppressants: X-axis represented different types of cancer, while Y-axis represented the gene symbol of immunosuppressants. (**E**), the correlation between immunestimulators RAET1E and OAS1 expression. (**F**), the correlation between immunestimulators IL6R and OAS1 expression. (**G**), the correlation between immunosuppressants LGALS9 and OAS1 expression. (**H**), the correlation between immunosuppressants ADORA2A and OAS1 expression

(GO:0045071; Genes: RNASEL, RSAD2, OAS1, OAS2, OAS3, MX1, ISG15, and IFIT1) (Fig. 5D) and KEGG pathways, including Hepatitis C (hsa05160; RNASEL, RSAD2, OAS1, STAT1, OAS2, OAS3, MX1, and IFIT1) (Fig. 5E).

### Transcription regulation analysis

TFs and miRNAs associated with OAS1 were predicted in this study. The result showed that a total of 1 TF (TF signal transducer and activator of transcription 3 [STAT3]), 34 miRNAs, OAS1 as well as TF-miRNA-gene interactions, such as STAT3-miR-21-OAS1, were finally investigated. The transcriptional regulatory network is shown in Fig. 6.

### OAS1 expression in patients with LUAD

Ten patients with LUAD were included in this study. Immunohistochemical staining revealed that the protein expression of OAS1 was higher in LUAD tissues than in the corresponding normal tissues ($p<0.05$). Differential OAS1 expression levels are shown in Fig. 7A. As shown in Fig. 7B, the number of CD68 positive M1 macrophages

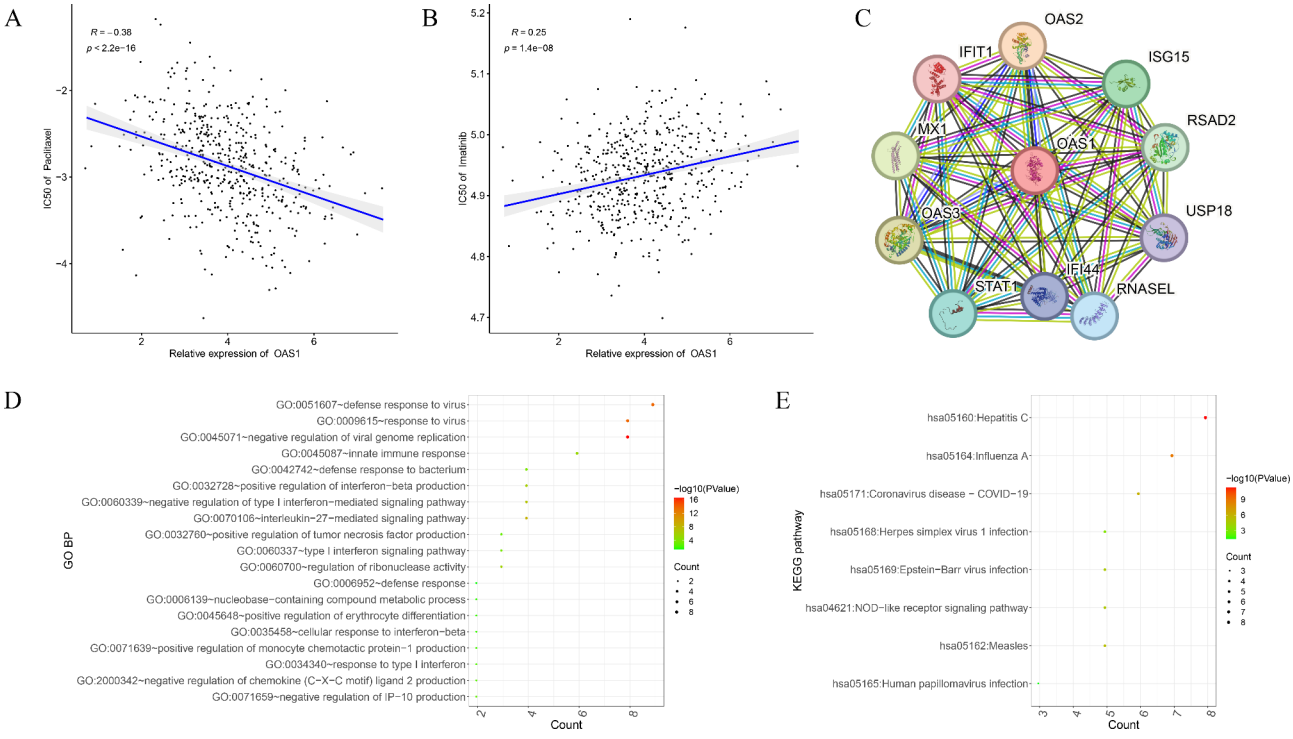


**Fig. 5** Drug and PPI network analysis for OAS1. (**A**), Scatter plot of correlation between IC50 and OAS1 expression in Paclitaxel. (**B**), Scatter plot of correlation between IC50 and OAS1 expression in Imatinib. (**C**), the PPI network constructed by OAS1 and associated proteins: the node represented genes, while the line between two nodes represented interactions. (**D**), the significant GO-BP functions assembled by OAS1 and associated genes: the bigger the nod, the more genes assembled in certain function; the redder the color, the smaller the P value. (**E**), the significant KEGG pathways enriched by OAS1 and associated genes: the bigger the nod, the more genes enriched in certain pathway; the redder the color, the smaller the P value

was obviously higher in the OAS1 high-expression group than in the low-expression group, indicating high infiltration of M1 macrophages in the OAS1 high-expression group.

### Role of OAS1 expression in LUAD cell lines

The relative mRNA expression of OAS1 in the four LUAD cell lines and in normal cells (control) was investigated using RT-qPCR. The results showed that the expression of OAS1 in all four cell lines (A549, NCI-H78, NCI-H102, and BL2195) was significantly higher than that in the controls (all $P<0.05$). OAS1 expression in the verification analysis was in accordance with the findings of this bioinformatics study, confirming the reliability of our results. A bar chart depicting OAS1 expression in the cell lines and the control group is presented in Fig. 8A. Western blotting verified the overexpression of OAS1 in A549 and NCI-H78 LUAD cell lines compared to that in the controls (Fig. 8B). To determine the role of OAS1 in LUAD, OAS1 expression was knocked down using siRNA. The high transfection efficiency is shown in Fig. 8C. CCK8 assay showed that the viability of si-OAS1-transfected cells was significantly lower than that of the control cells ($p<0.05$). The colony formation assay suggested that the ability of A549 cells to form colonies was significantly suppressed in the si-OAS1 group ($p<0.05$; Fig. 8D). In addition, OAS1 knockdown effectively inhibited the migration of A549 cells ($P<0.05$; Fig. 8E). These results indicate that aberrantly high OAS1 expression contributes to LUAD tumorigenesis.

### Expression of STAT3 and miR-21 in LUAD cells

With respect to the STAT3-miR-21-OAS1 interaction identified in the transcriptional regulation network, the expression levels of STAT3 and miR-21 were determined in LUAD cells. The results showed that STAT3 was overexpressed, while miR-21 was downregulated in A549 cells compared to that in the normal bronchial epithelial cell line BEAS-2B ($p<0.05$, Fig. 9).

## Discussion

LUAD is the most frequent subtype of lung cancer, with a poor survival rate due to a limited understanding of its pathological mechanism and prognosis. Although OAS1 has proven to be valuable for the prognosis of various human cancers, research on its role in LUAD is rare. The present analysis revealed that the expression of OAS1 in LUAD samples was dramatically higher than that in normal samples. OAS1 upregulation is associated with poor prognosis, lymph node metastasis, and advanced

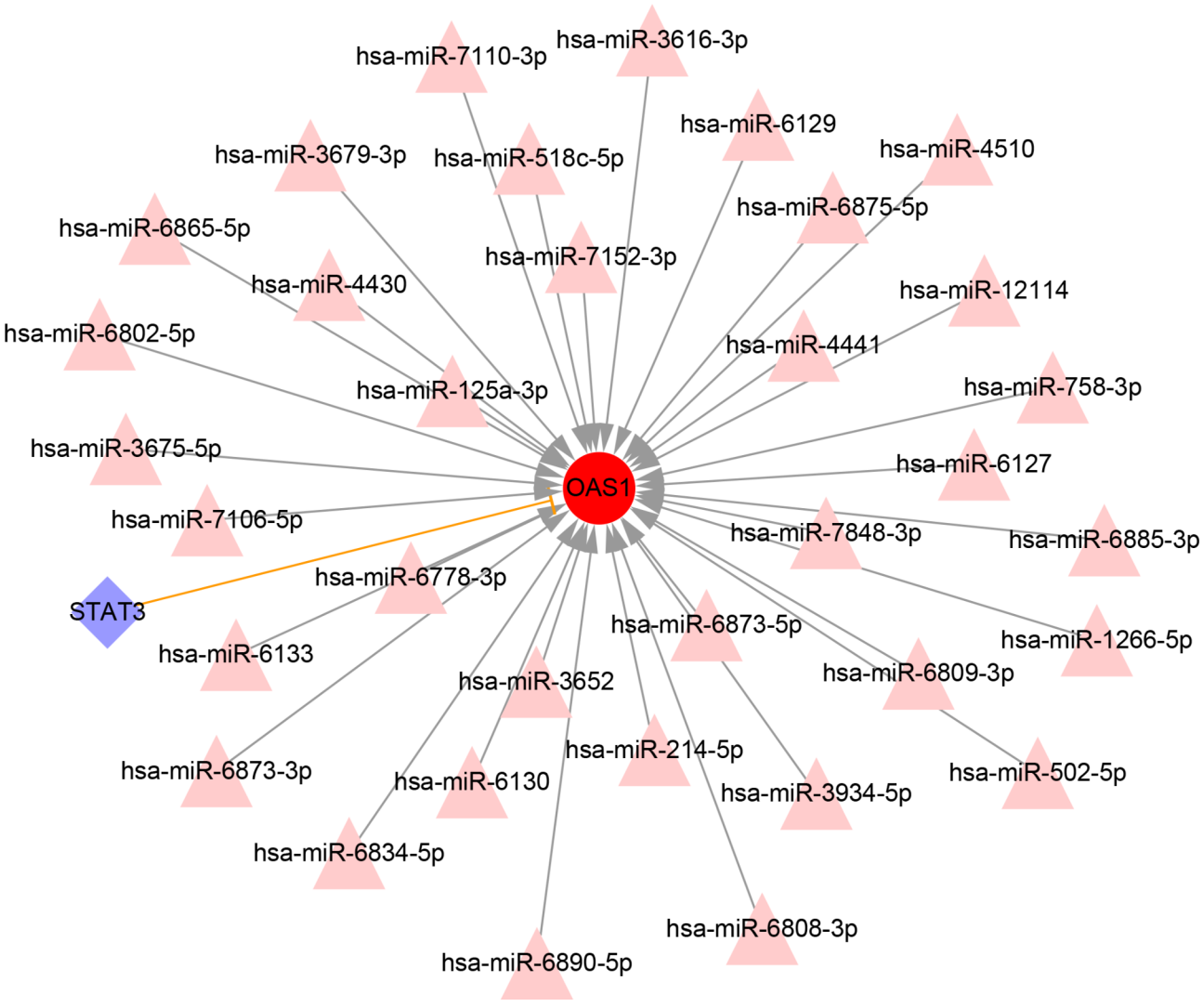


**Fig. 6** The regulatory network constructed by OAS1 and associated transcription factor (TF) and miRNA. The pink triangle represented miRNA; the purple diamond represented TF; the red circle represented OAS1; the gray arrow line indicated miRNA targeting OAS1, while the yellow T-shaped line indicated TF regulating OAS1.

tumor stage. Simultaneously, elevated OAS1 expression was positively correlated with immune cells (e.g., macrophages M0 and M1) and immunomodulators (e.g., IL6R). The prognostic value of OAS1 in LUAD was determined via univariate regression analysis. In total, 10 genes associated with OAS1 were revealed via PPI analysis, which were mainly enriched in functions, such as the negative regulation of viral genome replication. Transcriptional analysis revealed several OAS1-related interactions, including STAT3-miR-21-OAS1. Finally, qPCR analysis validated the expression of OAS1, confirming its consistency with the bioinformatics results.

Therefore, more reliable predictors for adequately characterizing the prognosis of human cancers, including LUAD, are essential [33]. A previous study identified a prognostic biomarker based on gene expression that enhanced the comprehension of LUAD prognostication [34]. In fact, the overexpression of certain genes is closely related to poor survival in human cancers, providing new insights for identifying prognostic genes [35]. The prognostic value of OAS1 for clinical intervention in breast cancer has already been proven as a gene that plays a vital role in antiviral immunity [36]. In a previous prognostic marker investigation, Lu et al. demonstrated that OAS1 exhibited higher expression levels in pancreatic cancer cells than in normal cells [10]. Furthermore, OAS1 overexpression was closely related to poor overall survival and advanced tumor stage, suggesting that OAS1 could serve as a valuable prognostic factor for cancer. Clinical characteristics, such as tumor stage and survival time, are commonly used to identify potential gene biomarkers for the clinical prognosis of lung cancer [37]. It

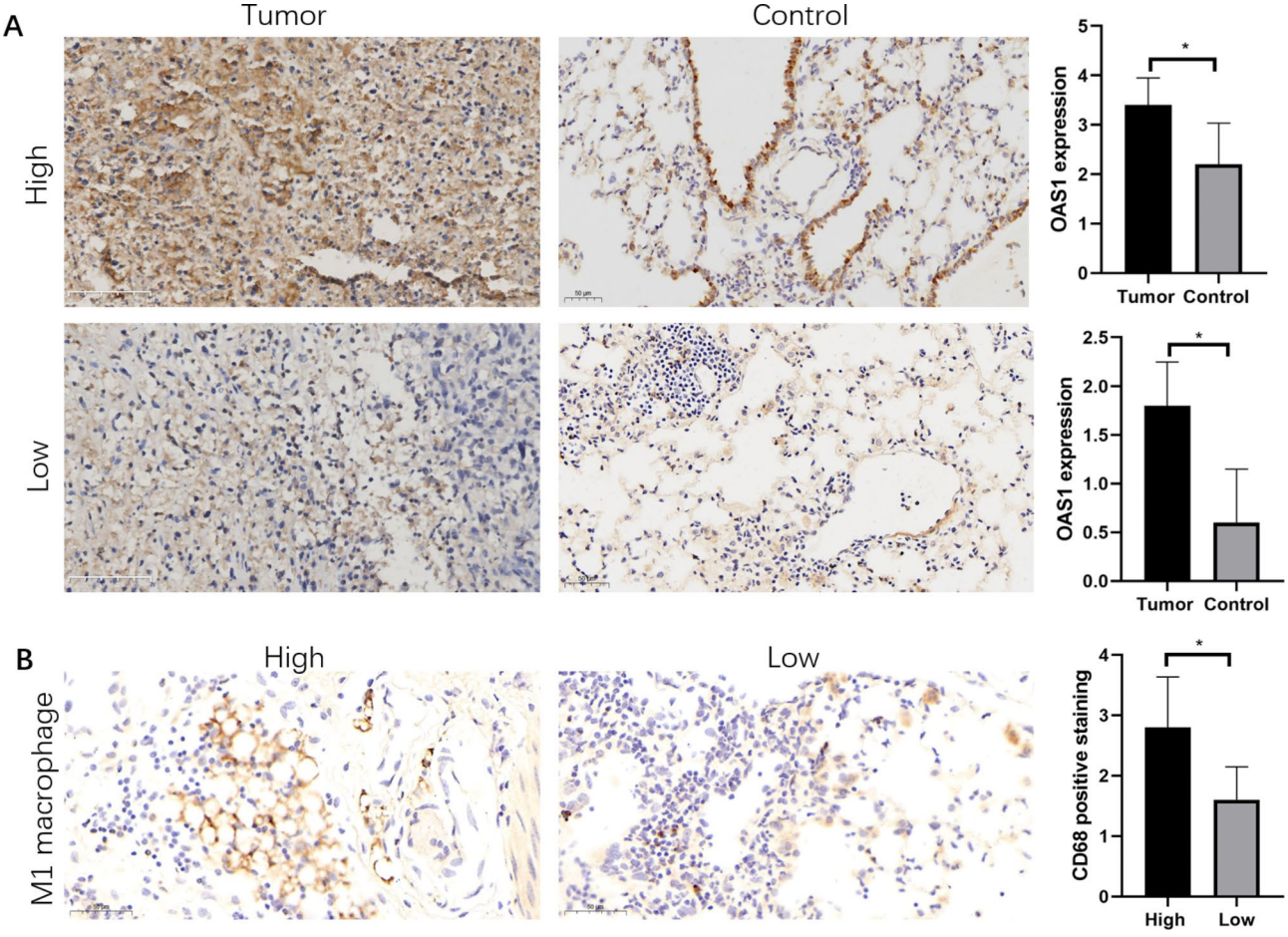


**Fig. 7** Immunohistochemical staining of OAS1 expression. (**A**), immunohistochemical staining of OAS1 in high and low expression group. (**B**), CD68 staining for M1 macrophage in tumor tissues of OAS1 high and low expression group $*p < 0.05$

has been shown that chemokine (C-C motif) ligand 19 (CCL19) has been linked to lymph node metastasis and an unfavorable prognosis in individuals with small cell lung cancer. Its expression promotes tumor progression and metastasis [38]. Importantly, the role of OAS1 in the survival and prognosis of human cancer may be closely related to its relationship with immune cells. Yu et al. indicated the downregulation of the macrophage M1-related gene OAS1 in bladder urothelial carcinoma cell lines, which proved that OAS1 affected the development, activity, and immune response of immune cells by acting on them and can be further used for disease prognosis [39]. Interleukin-6 receptor (IL6R), an immunostimulant gene involved in the development of human cancer, can activate immune cells and increase their activity, making it easy for them to recognize and attack cancer cells, ultimately leading to better disease control and longer survival [40]. In the current study, either OAS1 gene or protein was upregulated in patients with LUAD when compared to normal individuals. RT-qPCR confirmed OAS1 overexpression in LUAD cells. Importantly, OAS1 was correlated with poor prognosis, lymph node metastasis, advanced tumor stage, and the expression of immune cells, such as macrophages M1. This finding is consistent with those of previous studies and supports the role of OAS1 in the development and activity of immune cells. Thus, the results of the current analysis indicate that the expression of OAS1 might influence survival and immune cell expression in patients, making it a potential prognostic gene for LUAD. These results help explain the relationship between high OAS1 expression and unfavorable LUAD prognosis, providing new clues for the development of immunotherapy strategies.

Lung cancer exhibits both distinct and shared dysregulated genes and transcription factors that coexist and interact synergistically within a cohesive transcriptional regulatory network, potentially influencing vital pathways related to the acquisition of cancer hallmarks [41]. It has been proven that the TF-miRNA-mRNA regulatory relationship contributes to the prognosis of human cancers, including hepatocellular carcinoma, which may shed light on possible molecular mechanisms [42]. STAT3 plays a pivotal role in modulating the immune response against tumors. It exhibits extensive hyperactivity in

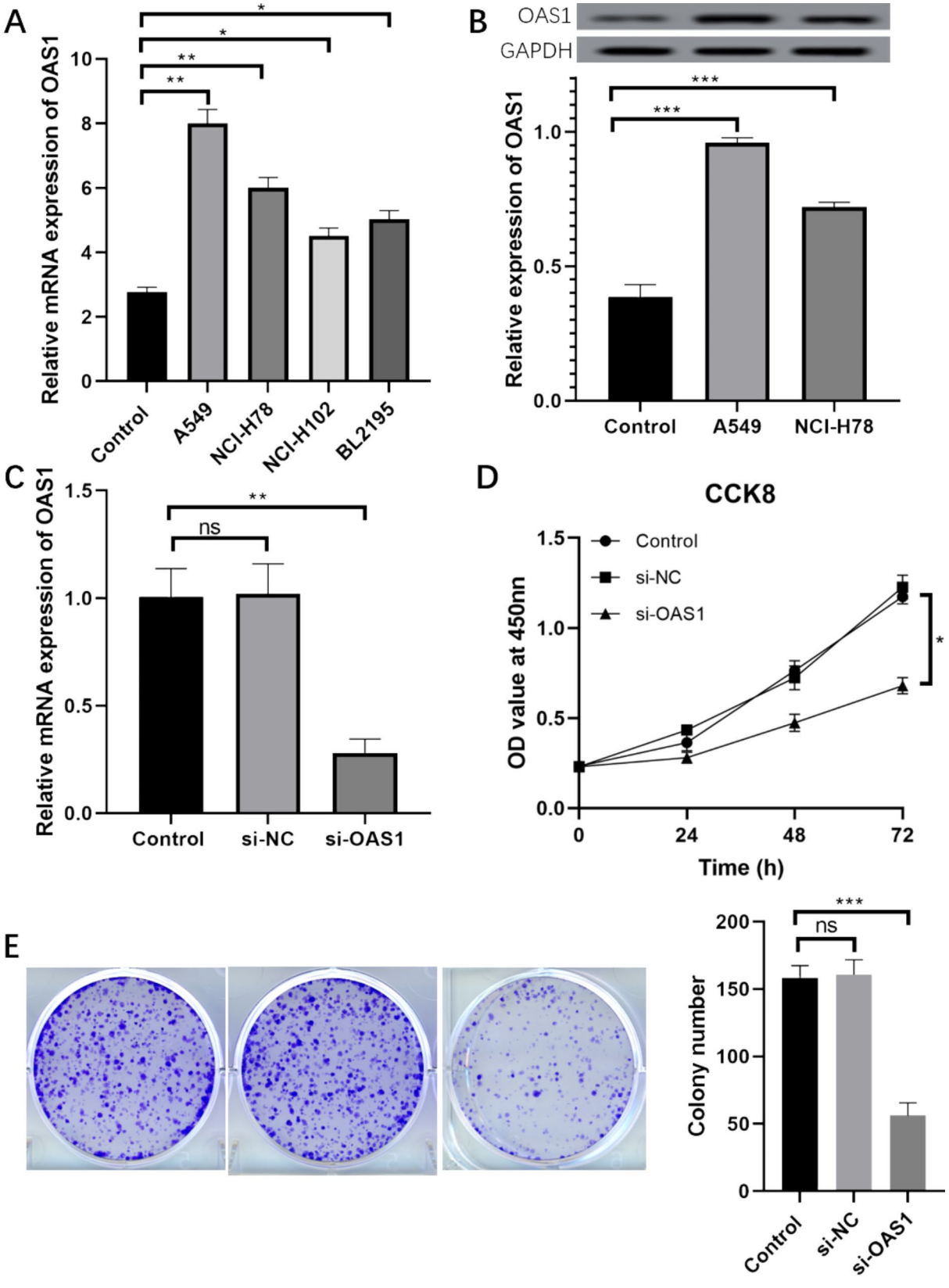


**Fig. 8** OAS1 knockdown suppressed A549 cell viability. (**A**), the expression of OAS1 in normal bronchial epithelial tissue cells (control) and four LUAD cell lines A549, NCI-H78, NCI-H102 and BL2195. (**B**), western blot for the expression of OAS1 in A549, NCI-H78 cell lines. (**C**), the transfection efficiency of si-OAS1 in A549 cells. (**D**), cell viability after si-OAS1 transfection. (**E**), colony formation assay after OAS1 knockdown. *$p < 0.05$, **$p < 0.01$, ***$p < 0.001$

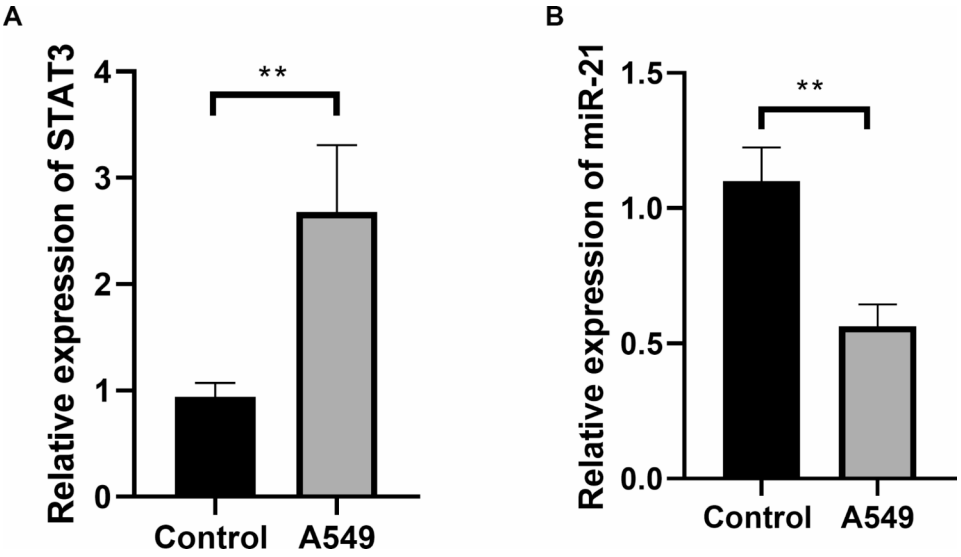


**Fig. 9** The expression of STAT3 and miR-21 in A549 cells. $^{**}p < 0.01$

both malignant and non-malignant cells present within the tumor microenvironment and plays a significant role in suppressing the expression of key immune activation regulators while fostering the generation of immunosuppressive factors [43]. The close relationship between STAT3 and lung cancer has been widely explored because it participates in the entire process of tumor occurrence and lung cancer development [44]. Zhao et al. demonstrated that cisplatin resistance in human LUAD cells can be achieved by modulating the miRNA/STAT3 axis [45]. MiR-21 is frequently regarded as a cancer-related miRNA because of its association with unregulated cell proliferation, resistance to apoptosis, and invasion and metastasis of lung cancer [46]. A previous study has established that miR-21, a potent therapeutic target for solid malignancies characterized by heightened STAT3 activity, plays a role in mediating the progression of inflammation-associated gastric cancer [47]. LUAD-derived exosomal miR-21 promotes osteoclastogenesis, indicating its potential as a therapeutic target for bone metastasis [48]. Yang et al. showed that the suppression of miR-21 contributes to osteoblast cell apoptosis through the upregulation of OAS1, which indicates the important role of the miR-21-OAS1 relationship in the progression of human disease [49]. Compelling evidence has shown that STAT3 is aberrantly activated in lung cancer [50, 51]. Our data showed that STAT3 was overexpressed in LUAD cells, which is consistent with the results of previous studies. In the present study, OAS1 was found to be vital for LUAD development. Our data showed that OAS1 knockdown impeded the proliferation and migration of LUAD cells, indicating the potential of OAS1 as a therapeutic target. Interestingly, transcriptional analysis revealed several OAS1-related interactions, including STAT3-miR-21-OAS1, which deserve further investigation. Thus, we speculate that OAS1 might contribute to the progression of LUAD by participating in the STAT3-miR-21-OAS1 axis, which warrants further analysis.

## Conclusion

In conclusion, the upregulation of OAS1 might influence patient survival and immune cell expression, making it a potential prognostic gene for LUAD. Moreover, OAS1 contributed to the progression of LUAD by participating in the STAT3-miR-21-OAS1 axis.

### Abbreviations

| | |
|---|---|
| OAS1 | Oligoadenylate synthetase 1 |
| LUAD | Lung adenocarcinoma |
| KM | Kaplan-Meier |
| GDSC | Cancer drug sensitivity Genomics |
| TFs | Transcription factors |
| RPMI | Roswell Park Memorial Institute |

## Supplementary Information

The online version contains supplementary material available at https://doi.org/10.1186/s12890-024-03206-3.

Supplementary Material 1

Supplementary Material 2

Supplementary Material 3

Supplementary Material 4

Supplementary Material 5

Supplementary Material 6

### Acknowledgements

Not applicable.

**Author contributions**
LW and LLG carried out the Conception and design of the research, FD and KG participated in the Acquisition of data. QL and XLY carried out the Analysis and interpretation of data. LW drafted the manuscript. XLY performed the revision of manuscript for important intellectual content. All authors reviewed the manuscript.

**Funding**
Not applicable.

**Data availability**
The datasets generated and/or analysed during the current study are available in the UCSC Xene database (http://cbioportal.org), and GEO database (including GSE31210 dataset (https://www.ncbi.nlm.nih.gov/gds/?term=GSE31210) and GSE68465 dataset (https://www.ncbi.nlm.nih.gov/gds/?term=GSE68465)).

## Declarations

**Ethics approval and consent to participate**
All participants provided written informed consent before commencement of the study. This study was approved by the Ethics Committee of Zibo Hospital of Integrated Traditional Chinese and Western Medicine (No.202211) and was conducted in accordance with the Declaration of Helsinki guidelines. This study was registered in Chictr.org.cn (https://www.chictr.org.cn/) with Clinical Trial Number of ChiCTR2400085823.

**Consent for publication**
Not applicable.

**Competing interests**
The authors declare no competing interests.

Received: 26 October 2023 / Accepted: 7 August 2024
Published online: 27 September 2024

**References**

1. Su L, Zhao J, Su H, Wang Y, Huang W, Jiang X, Gao S. CircRNAs in lung adenocarcinoma: diagnosis and therapy. Curr Gene Ther. 2022;22(1):15–22.
2. Borczuk AC. Updates in grading and invasion assessment in lung adenocarcinoma. Mod Pathology: Official J United States Can Acad Pathol Inc. 2022;35(Suppl 1):28–35.
3. Succony L, Rassl DM, Barker AP, McCaughan FM, Rintoul RC. Adenocarcinoma spectrum lesions of the lung: detection, pathology and treatment strategies. Cancer Treat Rev. 2021;99:102237.
4. Hutchinson BD, Shroff GS, Truong MT, Ko JP. Spectrum of Lung Adenocarcinoma. Semin Ultrasound CT MR. 2019;40(3):255–64.
5. Qi C, Ma J, Sun J, Wu X, Ding J. The role of molecular subtypes and immune infiltration characteristics based on disulfidptosis-associated genes in lung adenocarcinoma. Aging. 2023;15(11):5075–95.
6. Yu Y, Wang Z, Zheng Q, Li J. FAM72 serves as a biomarker of poor prognosis in human lung adenocarcinoma. Aging. 2021;13(6):8155–76.
7. Zengin T, Önal-Süzek T. Analysis of genomic and transcriptomic variations as prognostic signature for lung adenocarcinoma. BMC Bioinformatics. 2020;21(Suppl 14):368.
8. Magg T, Okano T, Koenig LM, Boehmer DFR, Schwartz SL, Inoue K, Heimall J, Licciardi F, Ley-Zaporozhan J, Ferdman RM et al. Heterozygous OAS1 gain-of-function variants cause an autoinflammatory immunodeficiency. Sci Immunol 2021, 6(60).
9. Li X, Shen Y, Xu X, Guo G, Chen Y, Wei Q, Li H, He K, Liu C. Genomic and RNA-Seq profiling of patients with HFrEF unraveled OAS1 mutation and aggressive expression. Int J Cardiol. 2023;375:44–54.
10. Lu L, Wang H, Fang J, Zheng J, Liu B, Xia L, Li D. Overexpression of OAS1 is correlated with poor prognosis in pancreatic Cancer. Front Oncol. 2022;12:944194.
11. Song C, Guo Z, Yu D, Wang Y, Wang Q, Dong Z, Hu W. A prognostic Nomogram Combining Immune-related gene signature and clinical factors predicts survival in patients with lung adenocarcinoma. Front Oncol. 2020;10:1300.
12. Sui Y, Li S, Fu XQ, Zhao ZJ, Xing S. Bioinformatics analyses of combined databases identify shared differentially expressed genes in cancer and autoimmune disease. J Translational Med. 2023;21(1):109.
13. Jin K, Qiu S, Jin D, Zhou X, Zheng X, Li J, Liao X, Yang L, Wei Q. Development of prognostic signature based on immune-related genes in muscle-invasive bladder cancer: bioinformatics analysis of TCGA database. Aging. 2021;13(2):1859–71.
14. Goldman MJ, Craft B, Hastie M, Repečka K, McDade F, Kamath A, Banerjee A, Luo Y, Rogers D, Brooks AN, et al. Visualizing and interpreting cancer genomics data via the Xena platform. Nat Biotechnol. 2020;38(6):675–8.
15. Okayama H, Kohno T, Ishii Y, Shimada Y, Shiraishi K, Iwakawa R, Furuta K, Tsuta K, Shibata T, Yamamoto S, et al. Identification of genes upregulated in ALK-positive and EGFR/KRAS/ALK-negative lung adenocarcinomas. Cancer Res. 2012;72(1):100–11.
16. Shedden K, Taylor JM, Enkemann SA, Tsao MS, Yeatman TJ, Gerald WL, Eschrich S, Jurisica I, Giordano TJ, Misek DE, et al. Gene expression-based survival prediction in lung adenocarcinoma: a multi-site, blinded validation study. Nat Med. 2008;14(8):822–7.
17. Ito K, Murphy D. Application of ggplot2 to Pharmacometric Graphics. CPT: Pharmacometrics Syst Pharmacol. 2013;2(10):e79.
18. Uhlén M, Fagerberg L, Hallström BM, Lindskog C, Oksvold P, Mardinoglu A, Sivertsson Å, Kampf C, Sjöstedt E, Asplund A. Tissue-based map of the human proteome. Science. 2015;347(6220):1260419.
19. Bland JM, Altman DG. Survival probabilities (the Kaplan-Meier method). BMJ. 1998;317(7172):1572.
20. Hänzelmann S, Castelo R, Guinney J. GSVA: gene set variation analysis for microarray and RNA-Seq data. BMC Bioinformatics. 2013;14(1):7.
21. Chen B, Khodadoust MS, Liu CL, Newman AM, Alizadeh AA. Profiling Tumor infiltrating Immune cells with CIBERSORT. Methods Mol Biol. 2018;1711:243–59.
22. Kawada JI, Takeuchi S, Imai H, Okumura T, Horiba K, Suzuki T, Torii Y, Yasuda K, Imanaka-Yoshida K, Ito Y. Immune cell infiltration landscapes in pediatric acute myocarditis analyzed by CIBERSORT. J Cardiol. 2021;77(2):174–8.
23. Ru B, Wong CN, Tong Y, Zhong JY, Zhong SSW, Wu WC, Chu KC, Wong CY, Lau CY, Chen I, et al. TISIDB: an integrated repository portal for tumor-immune system interactions. Bioinf (Oxford England). 2019;35(20):4200–2.
24. Mosmann T. Rapid colorimetric assay for cellular growth and survival: application to proliferation and cytotoxicity assays. J Immunol Methods. 1983;65(1–2):55–63.
25. Geeleher P, Cox N, Huang RS. pRRophetic: an R package for prediction of clinical chemotherapeutic response from tumor gene expression levels. PLoS ONE. 2014;9(9):e107468.
26. Shannon P, Markiel A, Ozier O, Baliga NS, Wang JT, Ramage D, Amin N, Schwikowski B, Ideker T. Cytoscape: a software environment for integrated models of biomolecular interaction networks. Genome Res. 2003;13(11):2498–504.
27. Dennis G Jr., Sherman BT, Hosack DA, Yang J, Gao W, Lane HC, Lempicki RA. DAVID: database for annotation, visualization, and Integrated Discovery. Genome Biol. 2003;4(5):P3.
28. Dweep H, Gretz N. miRWalk2.0: a comprehensive atlas of microRNA-target interactions. Nat Methods. 2015;12(8):697.
29. Wong N, Wang X. miRDB: an online resource for microRNA target prediction and functional annotations. Nucleic Acids Res. 2015;43(Database issue):D146.
30. Liberzon A, Subramanian A, Pinchback R, Thorvaldsdóttir H, Tamayo P, Mesirov JP. Molecular signatures database (MSigDB) 3.0. Bioinformatics. 2011;27(12):1739–40.
31. Tsuji Y, Kuramochi M, Golbar H, Izawa T, Kuwamura M, Yamate J. Acetaminophen-Induced Rat Hepatotoxicity based on M1/M2-Macrophage polarization, in possible relation to damage-Associated molecular patterns and Autophagy. Int J Mol Sci 2020, 21(23).
32. Livak KJST. Analysis of relative gene expression data using real-time quantitative PCR and the 2(-Delta Delta C(T))method. Methods. Dec; 2001;25(4):402–8.
33. Wu P, Zheng Y, Wang Y, Wang Y, Liang N. Development and validation of a robust immune-related prognostic signature in early-stage lung adenocarcinoma. J Translational Med. 2020;18(1):380.
34. Zhao J, Guo C, Ma Z, Liu H, Yang C, Li S. Identification of a novel gene expression signature associated with overall survival in patients with lung adenocarcinoma: a comprehensive analysis based on TCGA and GEO databases. Lung cancer (Amsterdam Netherlands). 2020;149:90–6.

35. Wu R, Patel A, Tokumaru Y, Asaoka M, Oshi M, Yan L, Ishikawa T, Takabe K. High RAD51 gene expression is associated with aggressive biology and with poor survival in breast cancer. Breast Cancer Res Treat. 2022;193(1):49–63.
36. Zhang Y, Yu C. Prognostic characterization of OAS1/OAS2/OAS3/OASL in breast cancer. BMC Cancer. 2020;20(1):575.
37. Peters BA, Pass HI, Burk RD, Xue X, Goparaju C, Sollecito CC, Grassi E, Segal LN, Tsay JJ, Hayes RB, et al. The lung microbiome, peripheral gene expression, and recurrence-free survival after resection of stage II non-small cell lung cancer. Genome Med. 2022;14(1):121.
38. Liu Q, Qiao M, Lohinai Z, Mao S, Pan Y, Wang Y, Yang S, Zhou F, Jiang T, Yi X, et al. CCL19 associates with lymph node metastasis and inferior prognosis in patients with small cell lung cancer. Lung Cancer. 2021;162:194–202.
39. Yu Y, Huang Y, Li C, Ou S, Xu C, Kang Z. Clinical value of M1 macrophage-related genes identification in bladder urothelial carcinoma and in vitro validation. Front Genet. 2022;13:1047004.
40. Wei X, Wang C, Feng H, Li B, Jiang P, Yang J, Zhu D, Zhang S, Jin T, Meng Y. Effects of ALOX5, IL6R and SFTPD gene polymorphisms on the risk of lung cancer: a case-control study in China. Int Immunopharmacol. 2020;79:106155.
41. Otálora-Otálora BA, López-Kleine L, Rojas A. Lung Cancer Gene Regulatory Network of Transcription Factors Related to the hallmarks of Cancer. Curr Issues Mol Biol. 2023;45(1):434–64.
42. Gao L, Xiong DD, He RQ, Lai ZF, Liu LM, Huang ZG, Yang X, Wu HY, Yang LH, Ma J, et al. Identifying TF-miRNA-mRNA regulatory modules in nitidine chloride treated HCC xenograft of nude mice. Am J Translational Res. 2019;11(12):7503–22.
43. Zou S, Tong Q, Liu B, Huang W, Tian Y, Fu X. Targeting STAT3 in Cancer Immunotherapy. Mol Cancer. 2020;19(1):145.
44. Zheng Q, Dong H, Mo J, Zhang Y, Huang J, Ouyang S, Shi S, Zhu K, Qu X, Hu W, et al. A novel STAT3 inhibitor W2014-S regresses human non-small cell lung cancer xenografts and sensitizes EGFR-TKI acquired resistance. Theranostics. 2021;11(2):824–40.
45. Zhao X, Li X, Zhou L, Ni J, Yan W, Ma R, Wu J, Feng J, Chen P. LncRNA HOXA11-AS drives cisplatin resistance of human LUAD cells via modulating miR-454-3p/Stat3. Cancer Sci. 2018;109(10):3068–79.
46. Rama AR, Quiñonero F, Mesas C, Melguizo C, Prados J. Synthetic circular miR-21 sponge as Tool for Lung Cancer Treatment. Int J Mol Sci 2022, 23(6).
47. Tse J, Pierce T, Carli ALE, Alorro MG, Thiem S, Marcusson EG, Ernst M, Buchert M. Onco-miR-21 promotes Stat3-Dependent gastric Cancer progression. Cancers 2022, 14(2).
48. Xu Z, Liu X, Wang H, Li J, Dai L, Li J, Dong C. Lung adenocarcinoma cell-derived exosomal miR-21 facilitates osteoclastogenesis. Gene. 2018;666:116–22.
49. Yang Y, Jiang J-S, Gao J-L. Low expression of microRNA-21 contributes to LPS-induced osteoblast cell apoptosis through up-regulation of OAS1. Cell LJ Biology m. 2015;61(5):68–73.
50. Dutta P, Sabri N, Li J, Li WX. Role of STAT3 in lung cancer. JAK-STAT. 2014;3(4):e999503.
51. Harada D, Takigawa N, Kiura K. The role of STAT3 in non-small cell lung cancer. Cancers (Basel). 2014;6(2):708–22.

## Publisher's Note

Springer Nature remains neutral with regard to jurisdictional claims in published maps and institutional affiliations.